Activation of Implanted Gold Markers in Therapeutic Proton Beams

J. J. Wilkens

Northeast Proton Therapy Center
Report Number 2004-01

January 2004

Activation of implanted gold markers in therapeutic proton beams

J. J. Wilkens[1,2], T. Bortfeld[1], J. M. Sisterson[1], E. Cascio[1]

1. *Northeast Proton Therapy Center, Massachusetts General Hospital, 30 Fruit Street, Boston MA 02114, USA*
2. *German Cancer Research Center (DKFZ), Department of Medical Physics, Im Neuenheimer Feld 280, 69120 Heidelberg, Germany*

Abstract

Implanted gold seeds are frequently used as markers for patient set-up in radiotherapy. In this work we study the activation of these gold seeds in clinical proton beams, and we investigate the potential use of this effect as an in vivo dosimeter. We irradiated gold seeds at the Northeast Proton Therapy Center in phantom experiments and measured the gamma spectra of the activated seeds with a germanium detector. Photopeaks from several gold isotopes with half-lives in the order of hours and days could be well identified in the spectra. The quantity of the different nuclides produced depended on the energy of the proton beam as well as on the fluence of secondary neutrons. The gamma energies were in the order of hundreds of keV and therefore high enough to be detected outside of the patient. However, in a clinical situation with four seeds and a dose of 2 Gy per fraction, the activities of the nuclides produced with the strongest signal would be of the order of a few becquerel, which are below the capabilities of common clinical instrumentation, preventing the application of this method in clinical practice.

KEYWORDS: proton therapy, gold seeds, activation.

1. INTRODUCTION

Implanted radiopaque marker seeds are clinically used for patient positioning and to assess target motion and set-up errors, mainly in prostate radiotherapy with X-rays [1-3], but also with protons [4]. Recent research on these markers was mostly directed to set-up and detection accuracy and seed migration [5-7].

But other interesting questions also arise in this context: the markers might influence the (local) dose distribution or the biological effect in the vicinity of the seeds due to secondary electrons produced in the gold, as it was reported for X-rays on tissue-metal interfaces [8, 9]. This might be even worse in proton beams, as neutrons and heavier charged secondaries like alpha particles can be produced in inelastic nuclear interactions. In general, nuclear interactions lead to an activation of the seeds, i.e. to the production of radioactive nuclides, including gamma emitters. The detection of their characteristic gamma-rays outside of the patient might be used for dosimetry and treatment verification, similar to positron emission tomography (PET) measurements of β^+ activity produced by proton beams interacting with light elements like carbon, nitrogen and oxygen [10, 11].

Therefore it is of interest to investigate the activation of gold seeds in clinical proton beams. In this paper, we will concentrate on gamma emitting reaction products and the production of gold isotopes. We will report their detection in two phantom experiments and we will evaluate the potential application as an *in vivo* dosimeter.

2. MATERIAL AND METHODS

We used cylindrical gold seeds with a length of 3 mm, a diameter of 0.8 mm and a purity of 99.9% ^{197}Au (Best Medical Inc.). We performed two qualitatively different experiments in the proton beams of the Northeast Proton Therapy Center (NPTC) at Massachusetts General Hospital: the first one was intended to investigate the generated isotopes and the corresponding cross sections, which was accomplished by using a very high fluence in a monoenergetic beam. The second experiment was designed to be of more clinical relevance, i.e. an appropriate clinical dose and a polyenergetic beam (spread-out Bragg peak, SOBP) were employed to simulate the situation of patient treatment.

Experiment I: High dose in monoenergetic beam.
This irradiation was carried out in the experimental beam line of the NPTC. Ten seeds were placed side by side in a plane perpendicular to the beam in a lucite holder behind 1.4 mm of lucite and a 76.2 µm Al monitor foil. A 230 MeV proton beam was widened by a lead scatter foil and collimated by a brass aperture (diameter 25 mm) to yield a homogeneous fluence (± 10%) over the area of the seeds. The mean energy at the surface of the seeds was 225 MeV. They were irradiated for 11 minutes with a total fluence of 10^{13} cm^{-2}, corresponding to a dose to water of about 6.7 kGy.

Experiment II: Clinical dose in spread-out Bragg peak.
For the second experiment, we used one of the gantry rooms of the NPTC. Ten seeds were placed in a $30 \cdot 30 \cdot 23$ cm^3 lucite phantom at a water equivalent depth of 19 cm. The proton beam was modulated to yield a SOBP with a range of 23 cm in water, a modulation width of 10 cm in water and a beam diameter of 12 cm, so that the seeds were almost in the centre of the SOBP. The seeds were irradiated with $2 \cdot 10^9$ protons per cm^2 with energies below 70 MeV to a dose to water of 3.74 Gy, which is still about a factor of 2 higher than a typical clinical dose per fraction.

In both cases, the seeds were removed from their phantoms after the irradiation and the spectrum of their gamma activity was measured at several times after irradiation using a high purity shielded Ge detector (Canberra Model GC1519 closed-end coaxial Ge detector, 50 mm diameter and 32 mm in length). The energy resolution of the detector was about 1.9 keV at 1.33 MeV. The energy dependent efficiency of the detector was calibrated with point sources and corrected for the counting geometry. The efficiency decreased rapidly for energies below ~100 keV, therefore while we can detect gamma-rays below 100 keV, the precise efficiency of their detection is unknown.

Ten unirradiated seeds were measured in the same geometry to obtain the background including detector noise, room background and any possible background from the unirradiated gold. The background spectrum consisted of some peaks, e.g. at 1461 keV from ^{40}K in the room, and a broad tail towards lower energies.

3. RESULTS

Figure 1 shows three spectra from experiment I, taken at different times after the irradiation. The signal is already corrected for the background and divided by the number of seeds. The spectrum consists of numerous lines, indicating that several radioactive isotopes have been produced. Most of the radionuclides produced decayed rapidly in the first few days, i.e. their half-lives are in the order of hours or days. The main features of the spectra and the strongest lines were below 700 keV, therefore the maximum energy in figure 1 was set to this value.

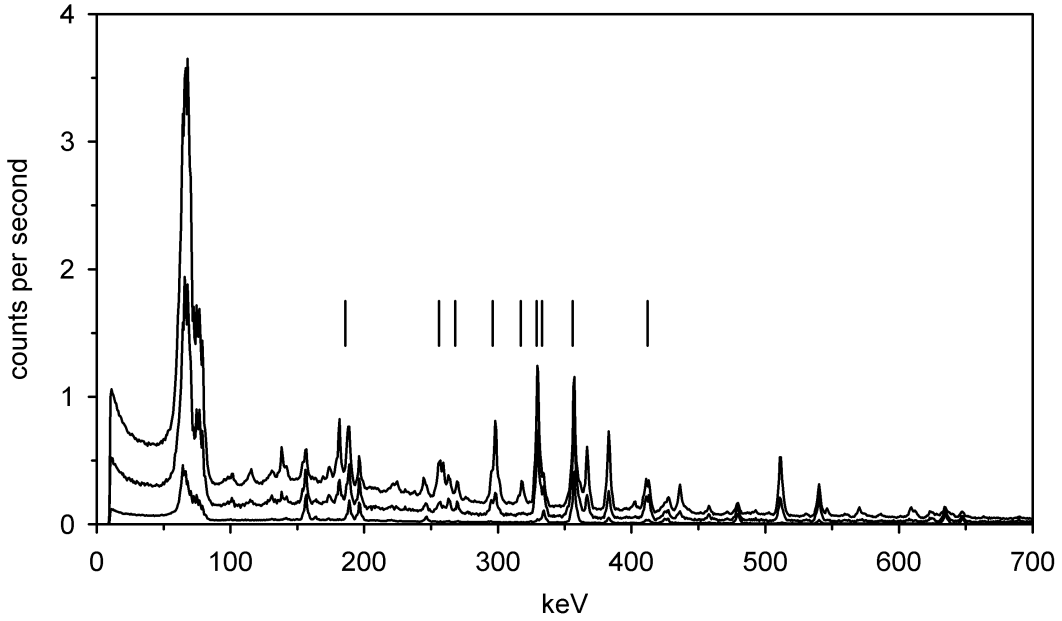

Figure 1: *Measured spectra per seed from experiment I (corrected for background). The three lines (top to bottom) correspond to measurements taken 45, 75 and 262 hours after irradiation. The counting times were 23, 5 and 63 minutes, respectively. The small vertical lines indicate the strongest gamma energies of some Au isotopes (cf. section 4).*

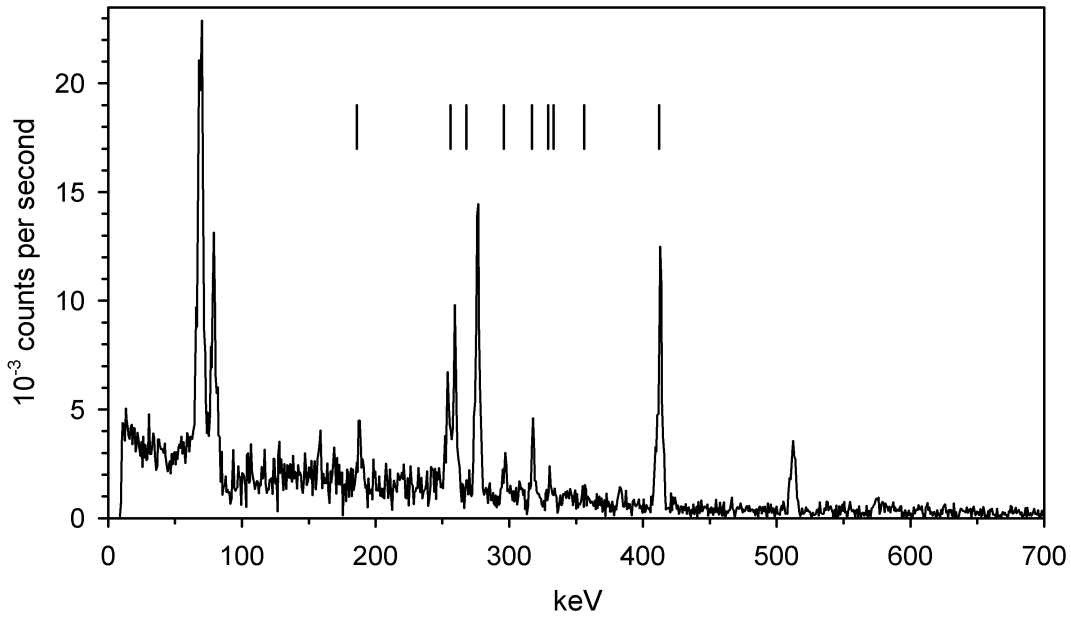

Figure 2: *Measured spectrum from experiment II in the gantry room (per seed, corrected for background). The measurement was started 0.5 hours after irradiation (counting time 1 hour). Again the small vertical lines indicate gamma energies from Au isotopes (cf. section 4).*

Results from experiment II are given in figure 2. In practical applications, the measurement would be done soon after the irradiation to obtain the highest possible signal. Therefore the measurement was started half an hour after the irradiation, with a counting time of one hour. The spectrum in figure 2 differs drastically from the spectra of the first experiment, which will be discussed in the following section. Table I shows some quantitative data for experiment II. Besides the total signal over all energies, two energy windows of interest were chosen to quantify the high signal in the low energy region (50-100 keV) and the strong and isolated peak at 412 keV (390-430 keV). The activities per seed in the respective energy windows at the time of the measurement were obtained by dividing the background corrected count rate by the efficiency of the detector.

Energy window (keV)	Count rate per seed (1/s) (corrected for background)	Total efficiency	Activity per seed (Bq)
1 - 3000	1.61 ± 0.02	-	-
50 - 100	0.355 ± 0.007	0.20 ± 0.02	1.8 ± 0.2
390 - 430	0.087 ± 0.003	0.053 ± 0.003	1.6 ± 0.1

Table I: *Count rates in some energy windows for experiment II (SOBP in the gantry room), obtained shortly after the irradiation (counting time 1 hour, started 0.5 hours after treatment). The total efficiency of the Ge detector (third column) was used to calculate the activity per seed in the respective energy windows.*

4. DISCUSSION

The analysis of the gamma spectra shows that several gamma emitting isotopes are produced in the gold. A detailed analysis regarding the nuclear reactions and the respective cross sections is currently under investigation. However, for the purpose of this paper a rough understanding of these processes is sufficient. In the spectra from the first experiment (figure 1), there is a high and broad peak below 100 keV, which seems to consist of at least two individual peaks. In the region above 100 keV, the photopeaks from several Au isotopes can be seen (^{192}Au, ^{193}Au, ^{194}Au, ^{196}Au and ^{198}Au), with the strongest peak from ^{194}Au at 328 keV. The most important gamma lines of these isotopes (table II) are indicated by the small vertical lines in figure 1.

Nuclide	Half-life	Strongest gamma lines in keV, intensity per disintegration in parentheses
^{192}Au	4.9 h	317 (0.58), 296 (0.22)
^{193}Au	17.7 h	186 (0.10), 256 (0.07), 268 (0.04)
^{194}Au	38.0 h	329 (0.60)
^{196}Au	6.2 d	356 (0.87), 333 (0.23)
^{198}Au	2.7 d	412 (0.96)

Table II: *Relevant Au isotopes, their half-lives and their most important gamma energies [12].*

The spectrum for experiment II (figure 2) showed some differences: Apart from the fact that the count rates are of course much smaller due to the lower dose, the spectrum has now a very strong photopeak from ^{198}Au at 412 keV, which is less pronounced in experiment I. ^{198}Au is produced from ^{197}Au by thermal neutrons, and the relative neutron fluence was much higher in the second experiment mainly due to neutrons generated in the phantom and somewhat due to the gantry beam line and the nozzle. The other variations between the two spectra can be attributed to the fact that the cross sections for nuclear reactions generally depend on the energy of the incident protons, which were quite different in the two experiments.

The half-lives of the Au isotopes (table II) are in the order of hours or days and are therefore considerably longer than the half-lives of radioactive nuclides produced in tissue, e.g. ^{11}C, ^{13}N and ^{15}O, which are used for PET during or shortly after treatment. This makes the Au isotopes suitable for off-line measurements, which could be scheduled a couple of hours after the irradiation when the short lived isotopes have already decayed.

We can now address the question whether the activation of the gold seeds might be used as an *in vivo* dosimeter. As the seeds would not be extracted from the patient after the irradiation, we have to measure the activation from outside the patient. From a clinical point a view, the easiest way would be to use an established detector system from nuclear medicine, e.g. an organ counter or a gamma camera, as they already provide a chair or couch and a 'patient friendly' environment.

To quantify the expected signal, one would have to pick one or more specific nuclear reactions, and use some kind of simulation to calculate the expected activity using the proton fluence within the patient and the relevant cross sections. Ideally, the simulation should even model attenuation and scattering of the gamma-rays from the seeds within the patient to get the estimated count rate in the detector. There are two energy regions that may be interesting because of their high count rates: the broad peak below 100 keV, and the line at 412 keV (cf. table I). But the low energy peak will have high attenuation in the patient (0.184 cm^{-1} in water at 80 keV [13]), and the activation will be difficult to predict as there are probably many reactions involved. Additionally, the background from Compton scatter is high in this region. The 412 keV line on the other hand is a single isolated peak and will have less attenuation in the patient (0.106 cm^{-1} at 400 keV [13]). However, it is a reaction initiated by neutrons, not protons, and the activation of the seed is therefore not a measure of the local dose, as the secondary neutrons may have traveled some distance in the patient before they interact with the gold.

To be of clinical use, the measured and the predicted signal have to be determined with an accuracy of a few percent. Otherwise, it would be difficult to base concrete clinical reactions on any observed deviations. For a realistic situation of a patient with four seeds and a dose per fraction of 2 Gy, one would get activities below 5 Bq for both the peak below 100 keV and the line at 412 keV (estimated from table I, assuming that the activation is proportional to the dose). Current clinical devices in nuclear medicine such as gamma cameras require at least tens or even hundreds of Bq in the body to detect and quantify a signal above background in a reasonable time of not more than 10-15 minutes [14, 15]. Even for whole-body counters in shielded chambers the minimum detectable activity (MDA) is of the order of tens of Bq ([16], p 58). Hence it stands to reason that our attempts to detect a signal from our seeds with a gamma camera failed.

Using gold seeds as an *in vivo* dosimeter is therefore not practical until improved techniques for the quantitative and accurate detection of such low activities in the body are available.

5. CONCLUSIONS

In principle, the activation of the gold seeds might be used a an *in vivo* dosimeter, as the half-lives and gamma energies of the produced isotopes are suitable for this procedure. However, the expected signal for therapeutic doses is very small (in the order of some Bq even for the strongest peaks), so the low signal-to-noise ratio makes it difficult to use this technique for dose verification. However, this experiment has verified that the total gamma activity of the seeds after treatment is fairly small, so the dose to the patient due to residual activity of the seeds will be negligible compared to the treatment dose.

The idea of using the activation of seeds as a dosimeter might work for a different material: the seeds do not necessarily have to be gold, as long as they are nontoxic and provide sufficient X-ray contrast on radiographs (if simultaneously used for positioning). If a material with much higher proton cross-sections for activation satisfies these requirements and still yields suitable radioactive nuclides in terms of half-lives and energies, the method might well find clinical applications.

6. ACKNOWLEDGMENTS

We would like to thank Drs Ali Bonab and Nathaniel Alpert (Department of Radiology, Massachusetts General Hospital) for helpful discussions and use of their equipment. This work has been supported in part by the National Cancer Institute program project grant CA21239: 'Proton radiation therapy research'. Jan J Wilkens was supported by the German Academic Exchange Service (DAAD Doktorandenstipendium).

7. REFERENCES

[1] Balter JM, Lam KL, Sandler HM, Littles JF, Bree RL, Ten Haken RK. Automated localization of the prostate at the time of treatment using implanted radiopaque markers: technical feasibility. Int. J. Radiat. Oncol. Biol. Phys. 1995:33; 1281-1286.

[2] Crook JM, Raymond Y, Salhani D, Yang H, Esche B. Prostate motion during standard radiotherapy as assessed by fiducial markers. Radiother. Oncol. 1995:37; 35-42.

[3] Nederveen AJ, Lagendijk JJW, Hofman P. Feasibility of automatic marker detection with an a-Si flat-panel imager. Phys. Med. Biol. 2001:46; 1219-1230.

[4] Rosenthal SJ, Wolfgang J. Targeting the prostate using on line imaging for proton therapy. Med. Phys. 2003:30; 1337.

[5] Litzenberg D, Dawson LA, Sandler H, Sanda MG, McShan DL, Ten Haken RK, Lam KL, Brock KK, Balter JM. Daily prostate targeting using implanted radiopaque markers. Int. J. Radiat. Oncol. Biol. Phys. 2002:52; 699-703.

[6] Dehnad H, Nederveen AJ, van der Heide UA, van Moorselaar RJA, Hofman P, Lagendijk JJW. Clinical feasibility study for the use of implanted gold seeds in the prostate as reliable positioning markers during megavoltage irradiation. Radiother. Oncol. 2003:67; 295-302.

[7] Pouliot J, Aubin M, Langen KM, Liu Y-M, Pickett B, Shinohara K, Roach M. (Non)-Migration of radiopaque markers used for on-line localization of the prostate with an electronic portal imaging device. Int. J. Radiat. Oncol. Biol. Phys. 2003:56; 862-866.

[8] Dutreix J, Bernard M. Dosimetry at interfaces for high energy X and gamma rays. Br. J. Radiol. 1966:39; 205-210.

[9] Regulla D, Panzer W, Schmid E, Stephan G, Harder D. Detection of elevated RBE in human lymphocytes exposed to secondary electrons released from x-irradiated metal surfaces. Radiat. Res. 2001:155; 744-747.

[10] Oelfke U, Lam GKY, Atkins MS. Proton dose monitoring with PET: quantitative studies in Lucite. Phys. Med. Biol. 1996:41; 177-196.

[11] Parodi K, Enghardt W, Haberer T. In-beam PET measurements of β^+ radioactivity induced by proton beams. Phys. Med. Biol. 2002:47; 21-36.

[12] Firestone RB. Table of Isotopes (vol II, 8th edition). Shirley VS et al. Ed. New York. John Wiley & Sons 1996.

[13] ICRU. Photon, Electron, Proton and Neutron Interaction Data for Body Tissues (ICRU report 46). Bethesda. International Commission on Radiation Units and Measurements 1992; 122.

[14] Nishiyama H, Lukes SJ, Saenger EL. Low-level internal radionuclide contamination: use of gamma camera for detection. Radiology 1984:150; 235-240.

[15] Wallström E, Alpsten M, Mattson S. A gamma camera for measurements of internal contamination after a radiological accident. J. Radiol. Prot. 1999:19; 143-154.

[16] ICRU. Direct determination of the body content of radionuclides (ICRU report 69). Journal of the ICRU 2003:3; 1-128.